

Casein hydrolysate diet controls intestinal T cell activation, free radical production and microbial colonisation in NOD mice

R. Emani · M. N. Asghar · R. Toivonen · L. Lauren ·
M. Söderström · D. M. Toivola · E. A. F. van Tol ·
A. Hänninen

Received: 8 January 2013 / Accepted: 30 April 2013 / Published online: 8 June 2013
© Springer-Verlag Berlin Heidelberg 2013

Abstract

Aims/hypothesis Dietary and microbial factors and the gut immune system are important in autoimmune diabetes. We evaluated inflammatory activity in the whole gut in prediabetic NOD mice using ex vivo imaging of reactive oxygen and nitrogen species (RONS), and correlated this with the above-mentioned factors.

Methods NOD mice were fed a normal diet or an anti-diabetogenic casein hydrolysate (CH) diet. RONS activity was detected by chemiluminescence imaging of the whole gut. Proinflammatory and T cell cytokines were studied in the gut and islets, and dietary effects on gut microbiota and short-chain fatty acids were determined.

Results Prediabetic NOD mice displayed high RONS activity in the epithelial cells of the distal small intestine, in conjunction with a proinflammatory cytokine profile. RONS production was effectively reduced by the CH diet, which also controlled (1) the expression of proinflammatory cytokines and colonisation-dependent *RegIII γ* (also known as *Reg3g*) in ileum; (2) intestinal T cell activation; and (3)

islet cytokines. The CH diet diminished microbial colonisation, increased the Bacteroidetes:Firmicutes ratio, and reduced lactic acid and butyric acid production in the gut.

Conclusions/interpretation Epithelial RONS production and proinflammatory T cell activation appears in the ileum of NOD mice after weaning to normal laboratory chow, but not after weaning to an anti-diabetogenic CH diet. Our data suggest a link between dietary factors, microbial colonisation and mucosal immune activation in NOD mice.

Keywords Casein hydrolysate · Dietary intervention · Guanine and cytosine profiling · Gut immune system · In vivo imaging system · Laser capture microscopy · Microbiota analysis · Nonobese diabetic (NOD) mouse · Reactive oxygen and nitrogen species · Type 1 diabetes

Abbreviations

| | |
|----------------|--------------------------------------|
| BB | Biobreeding |
| CH | Casein hydrolysate |
| DHE | Dihydroethidium |
| IVIS | In vivo imaging system |
| NF- κ B | Nuclear factor κ B |
| qPCR | Quantitative real-time PCR |
| RONS | Reactive oxygen and nitrogen species |
| ROS | Reactive oxygen species |
| SFB | Segmented filamentous bacteria |

Electronic supplementary material The online version of this article (doi:10.1007/s00125-013-2941-x) contains peer-reviewed but unedited supplementary material, which is available to authorised users.

R. Emani · R. Toivonen · L. Lauren · A. Hänninen (✉)
Department of Medical Microbiology and Immunology,
Kiinamyllynkatu 13,
FIN-20520 Turku, Finland
e-mail: arno.hanninen@utu.fi

M. N. Asghar · D. M. Toivola
Department of Bioscience/Cell Biology, Åbo Academy University,
Turku, Finland

M. Söderström
Department of Pathology, University of Turku, Turku, Finland

E. A. F. van Tol
Mead Johnson Nutrition, Nijmegen, the Netherlands

Introduction

One of the key environmental influences on the initiation and development of type 1 diabetes is thought to be microbial and nutritional factors. Epidemiological studies point to several candidate constituents of early nutrition as potential diabetes-triggering factors, including wheat proteins [1, 2],

cow's milk proteins [3, 4], alimentary roots and berries [5], and, although disputed, too low intake of vitamin D [6]. Recent investigations into gut microbiota have revealed qualitative differences in the composition of bacterial species between children who develop and those who do not develop type 1 diabetes [7, 8]. Both nutritional and microbial factors affect the homeostasis of the gastrointestinal tract and the gut immune system [9]. According to a plausible scenario, the cumulative effects of (1) an imbalanced microbiota and possible microbial insults to the gut, (2) intolerance to dietary proteins and (3) increased gut permeability synergistically predispose to an inflammatory tendency in the gut [10]. In a genetically predisposed host, this could lower the threshold of gut immune responses harmful to pancreatic islets.

Precisely how and where in the intestine this scenario promotes immune responses harmful to islets is not completely understood. Dietary factors are mostly digested and absorbed in the jejunum, biopsies from which have shown ultrastructural changes [11] and immunological markers [12] related to increased permeability and immune activation. In the biobreeding (BB) rat and the NOD mouse, diabetes penetrance is influenced by dietary factors [1], with reported impairment of epithelial barrier function in the small intestine [13, 14]. On the other hand, NOD mice show diet-dependent crypt hyperplasia and elevated levels of inflammatory cytokines in the large intestine [15]. T cell differentiation into regulatory or proinflammatory subsets in the large intestine is regulated by commensal microbiota [16–18], while the composition of microbiota appears to regulate autoimmunity in diabetes [7, 19, 20]. Thus, inflammation or defective immunoregulation in varying locations of the gut may converge through various functional and anatomical routes [21–23] to lead to autoimmunity in pancreatic lymph nodes and the islet environment.

Reactive oxygen and nitrogen species (RONS) are important in antimicrobial defence through their production in phagocytic leucocytes [24]. In addition, RONS regulate intracellular protein tyrosine kinases, which are important in immune responses [25], and activate cytokine production via nuclear factor κ B (NF- κ B) [26]. Using a sensitive chemiluminescence camera system, RONS can be detected from the whole animal with a RONS-sensitive probe (L-012) [27]. In models of experimental arthritis [27], systemic autoimmune disease [28] and bacterial colitis [29], whole-animal chemiluminescence imaging has been used to evaluate the level of inflammation in joints and other areas of anaesthetised mice.

To evaluate spatial and temporal aspects of inflammation in the gut of prediabetic NOD mice, we used *in vivo* and *ex vivo* imaging for RONS in live NOD mice and whole mouse intestine, respectively. Our results revealed increased free radical activity in the distal small intestine of prediabetic

NOD mice, which coincides with local production of proinflammatory cytokines and Th17-cell activation. These phenomena appear to depend on a diabetes-promoting diet and microbial colonisation of the gut, and involve impaired epithelial barrier function.

Methods

Mice and treatment groups NOD (NOD/ShiLtJ) mice were originally purchased from Jackson Laboratories (Bar Harbor, ME, USA), and bred and maintained in the local animal facility. For initial evaluation of inflammatory phenomena in the gut of NOD mice, we used age-matched female BALB/c mice as healthy control mice. BALB/c mice were kept on regular chow (SDS, Witham, UK) if not otherwise stated, whereas NOD mice were kept either on regular chow or a casein hydrolysate (CH)-containing dietary formulation (Nutramigen; Mead Johnson Nutrition, Glenview, IL, USA), starting at the time of weaning. Blood glucose was determined by tail vein puncture, with two consecutive readings over 14.3 mmol/l being considered to indicate diabetes. All experiments were subjected to rules of the National Board of Animal Experimentation in Finland and performed under license ESLH-2009-02371/Ym-23. The Principles of Laboratory Animal Care (<http://grants1.nih.gov/grants/olaw/references/phspol.htm>) were followed.

Determination of RONS production with chemiluminescence imaging The chemiluminescent probe L-012 (Wako Chemicals, Richmond, VA, USA) is a luminol derivative, which emits light when modified by reactive oxygen species (ROS) or reactive nitrogen species. The L012 probe was administered intraperitoneally at 50 mg/kg body weight in saline. For *in vivo* imaging, mice were anaesthetised with isoflurane and placed under an *in vivo* imaging system (IVIS)-100 (Xenogen, Alameda, CA, USA) camera for imaging. Images were taken at 1 to 5 min intervals until 30 min. For quantification of the emitted signal, region of interest values were recorded for each mouse from the abdominal area. For *ex vivo* imaging, mice were killed by CO₂ administration after intraperitoneal injection of L-012, and the whole gut was dissected and placed on a Petri-dish. Series of images were taken similarly to *in vivo* recordings and the emitted signal quantified using region of interest values.

Gut permeability measurements To evaluate intestinal barrier integrity, dextran uptake and systemic availability were assessed. Mice were given an intragastric bolus of 40 kDa dextran conjugated to FITC (FITC-Dextran 4; Sigma-Aldrich, St Louis, MO, USA), using a feeding needle. After 4 h, mice were killed and blood was collected by

cardiac puncture. Serum samples (70 μ l) were placed in duplicates in flat-bottomed 96-well plates (Immulon; Thermo Fisher, Waltham, MA, USA) and fluorescence was measured at 485 nm excitation (VictorPerkin Elmer, Waltham, MA, USA).

RNA isolation and quantitative real-time PCR Ileum samples were immersed in RNAlater (Qiagen, Hilden, Germany) immediately after dissection. Subsequently, RNA isolation was performed by homogenising samples with Power Lyser (MoBio, Carlsbad, CA, USA) and using ultra clean tissue and a cell RNA isolation kit (Power Lyser; MoBio). cDNA was synthesised with Maxima reverse transcriptase (Fermentas, St Leon-Rot, Germany). Cytokine expression was assessed by quantitative real-time PCR (qPCR) with light cycler 480 (Roche, Basel, Switzerland). Primer sequences are given in electronic supplementary material (ESM) Table 1. Absolute copy numbers of RNA (molecules/ μ g) were calculated by running standards and glyceraldehyde-3-phosphate dehydrogenase (*GAPDH*) as loading control. Analysis was performed using GraphPad Prism 5 (GraphPad Software, La Jolla, CA, USA).

Analysis of intestinal microbiota and short-chain fatty acids Intestinal microbiota composition and fatty acid profiles were analysed by Alimetrix (Espoo, Finland). Briefly, for evaluation of qualitative traits of total microbiota, bacterial chromosomal DNA was isolated from pooled caecal and colonic contents, and total bacterial chromosomal DNA stratified on the basis of guanine and cytosine (G+C) nucleotide content. In per cent G+C profiling, each of the pooled DNA samples was fractionated by 72 h CsCl equilibrium density gradient ultracentrifugation (100,000 g), which separates chromosomes with different G+C. In the following ultracentrifugation, the formed gradients were pumped through a flow-through UV absorbance detector set to 280 nm. This allowed PCR-independent profiling of dominant microbiota present in the samples. Subsequently, qPCR was applied using primer pairs specific to 16S rRNA-encoding sequences of six different clusters of bacteria: (1) Clostridial clusters IV and (2) XIVA; (3) *Bacteroides* spp.; (4) *Bifidobacterium* spp.; (5) *Lactobacillus* spp.; and (6) Coriobacteriaceae family. For quantification of total eubacterial numbers, primers targeting the conserved regions of 16S rRNA gene were applied. The bacterial numbers were calculated as 16S rRNA gene copy numbers per weight of content. In addition, the colonisation of segmented filamentous (SFB) bacteria was evaluated from three consecutive stool samples (ESM Table 2) by PCR after DNA isolation using a kit (FastDNA Spin kit for Soil; MP Biomedicals, Santa Ana, CA, USA) and a homogeniser (MagNA Lyser; Roche). Short-chain fatty acids were measured by gas chromatography using pivalic acid as an internal standard.

Gut histology and determination of epithelial cell RONS production For conventional histology, pieces of ileum were fixed in formalin and embedded in paraffin. Sections were stained with haematoxylin and eosin according to standard protocols. For detection of myeloperoxidase-containing cells, 5- to 7- μ m cryosections were fixed in acetone at -20°C and stained using anti-myeloperoxidase antibody (Ab-1; Thermo Fisher Scientific) and Alexa488-conjugated donkey-anti-rabbit Ig (Invitrogen, Carlsbad, CA, USA). Samples were imaged with confocal microscopy (Leica TCS SP5 Matrix, Wetzlar, Germany). Epithelial cell RONS production was determined using in vivo staining with dihydroethidium (DHE; Invitrogen). Briefly, mice were anaesthetised with ketamine (Pfizer, New York City, NY, USA) and xylazine (OrionPharma, Espoo, Finland), and their small intestine was exposed via a small incision in the abdominal skin and peritoneal cavity. DHE (200 μ l at 5 μ mol/l in PBS) was injected into the lumen of the ileum and mice were killed 20 min later. Dissected ileum samples were snap-frozen, processed for histochemistry, counterstained with DAPI (Invitrogen) and viewed under a UV microscope (Olympus, BX51, Berlin, Germany).

Flow cytometry of gut T cells Ileum samples were disrupted using collagenase (0.5 mg/ml, type VIII; Sigma) digestion and mechanical disruption to isolate lymphocytes from the lamina propria and epithelial layer. Mononuclear cells were further enriched using gradient centrifugation at room temperature for 20 min at 1,200 g with Lympholyte (Cedarlane, Burlington, ON, Canada) as described by the manufacturer. Cells were stained with FITC-conjugated anti-CD4 (Immunotools, Friesoythe, Germany) and phycoerythrin-conjugated anti-CD69 antibodies (BD Bioscience, Franklin Lakes, NJ, USA). Samples were run on a FACS Calibur flow cytometer and analysed with Cell Quest software (BD Bioscience).

T cell cytokine profiles in gut-draining lymph nodes Isolated mesenteric lymph node cells were stimulated with plate-bound anti-CD3 (eBiosciences, San Diego, CA, USA) in complete medium (DMEM with 10% (vol./vol.) FBS, L-glutamine 2 mmol/l, 100 U/ml penicillin plus streptomycin). Briefly, flat-bottomed 96-well plates (Nunc, Roskilde, Denmark) were pre-coated with anti-CD3. After removing unbound antibody, 1.0 million lymph node cells were plated in each well in duplicate in 200 μ l of complete medium. Supernatant fractions were collected 48 h later for cytokine analysis.

T cell cytokine secretion in response to CD3 stimulation was measured with multiplex cytokine bead array (FlowCytomix; eBioscience) using specific beads for each cytokine, anti-cytokine and phycoerythrin-conjugated antibody, and a protocol and software provided by the manufacturer.

Laser capture microscopy and isolation of islet RNA for cytokine profiling Pancreases were collected from 6-week-old mice. Frozen sections (16 μm thick) were cut on to nuclease-free PEN glasses (Zeiss, Oberkochen, Germany). The sections were stained with haematoxylin and eosin (Sigma) to visualise pancreatic islets. Islets were identified and scored for insulinitis under laser capture microscopy using a photo-activated localisation microscopy (PALM) device (Zeiss). Islets were encircled and cut with a UV laser, and automatically catapulted into an adhesive cap. All infiltrated islets from 30 to 50 sections per pancreas for each sample were collected. RNA was extracted from the laser capture microscopy samples using a kit (ArrayPure Nanoscale RNA Purification; Epicentre, Madison, WI, USA) for qPCR.

Statistical analyses The statistical significance of differences between groups was evaluated using unpaired Student's *t* test with Welch's correction or two-way ANOVA with post-hoc test for comparisons of more than two groups. The difference in diabetes incidence was evaluated using the Mann–Whitney *U* test. Statistical significance was accepted at $*p < 0.05$, $**p < 0.01$ and $***p < 0.001$.

Results

NOD mice on a diabetes-permissive chow diet have high in vivo RONS activity We imaged live NOD mice of various age groups with a chemiluminescence camera (IVIS) in order to evaluate whether enteropathy and gut immune system activation in NOD mice are associated with increased free radical activity, which is detectable in vivo as with joint inflammation [27]. Following intraperitoneal injection of the RONS-sensitive probe L-012, NOD mice emitted a signal from the abdominal area, which was significantly stronger than in healthy control BALB/c mice (Fig. 1a). This was true in every age group tested, i.e. in 5-, 7-, 12- and 20-week-old animals, with significance for the difference between NOD and BALB/c mice of all ages at $p < 0.001$ (Fig. 1b–e). We also weaned NOD female pups at 3 weeks of age to the anti-diabetogenic CH diet to determine whether a lack of dietary factors that promote diabetes would diminish RONS production. We further included a crossover group of mice, which was weaned to hydrolysate and then changed to normal chow later on, at 12 weeks of age (Fig. 1b–e). Free access was given to the CH diet, which allowed normal growth and weight gain (ESM Table 3). In these experiments, all mice on normal diet became diabetic, whereas 60% of mice on the CH diet (and in the crossover group) became diabetic (Fig. 1f). The CH diet efficiently reduced RONS production (Fig. 1b–e) in all age groups. A change to normal chow at a mature age resulted in only minimal upregulation of RONS production (Fig. 1e) and no

increase in diabetes incidence compared with mice on a continuous anti-diabetogenic (CH-based) diet (Fig. 1f).

Ex vivo imaging of the whole intestine revealed high RONS production in the distal small intestine of NOD mice We first addressed the possibility that peritoneal leucocytes were responsible for the RONS signal detected in vivo, but found this not to be the case (data not shown). Due to enteropathy and activation of the gut immune system in NOD mice, it was particularly important to determine whether the RONS signal detected in NOD mice originates from the gut and whether it is localised to any particular region of the gut. Ex vivo imaging of abdominal organs, including liver, spleen and pancreas, showed that no RONS signal was emitted from these organs. In contrast, imaging of the whole small and large intestine revealed various levels of signal from the gut, the highest levels being emitted from the distal small intestine, corresponding to the ileum (Fig. 1g). While newly weaned 3-week-old NOD intestines were almost completely devoid of a RONS signal, RONS levels in the ileum were high as early as 2 weeks later. Also in healthy BALB/c mice, the ileum emitted a stronger signal than other parts of the intestine. The CH diet reduced the level of the RONS-derived signal in the ileum of NOD mice, suggesting that regulation of RONS production is diet-dependent (Fig. 1h). Thus, RONS production seemed to be induced only after weaning to a normal chow-based diet.

As individual NOD mice showed different levels of RONS in their intestine, we determined whether RONS levels correlated with levels of insulinitis in the pancreas. High levels of RONS correlated with more advanced insulinitis, indicating an interdependence between intestinal RONS and insulinitis (Fig. 2).

To address the question of whether increased RONS production is associated with inflammation and also possibly further disrupts epithelial barrier function, we tested barrier function by intragastric gavage with FITC-dextran. While healthy BALB/c mice showed low or undetectable absorption of FITC-dextran into the circulation beyond 5 weeks of age, the majority of NOD mice had readily measurable serum levels at 6 or 8 weeks of age, with these levels being maintained at least until 10 to 12 weeks of age (Fig. 3a). NOD mice on the CH diet had markedly lower FITC-dextran absorption and differed significantly from control NOD mice at 10 to 12 weeks of age. In contrast, individual differences in RONS production did not correlate with FITC-dextran absorption (Fig. 3b,c). Thus, RONS production in NOD mice is not directly connected to gut barrier function in NOD mice.

RONS in the distal small intestine are produced by epithelial cells RONS are produced by myeloid cells such as neutrophils and macrophages in response to microbial contacts and

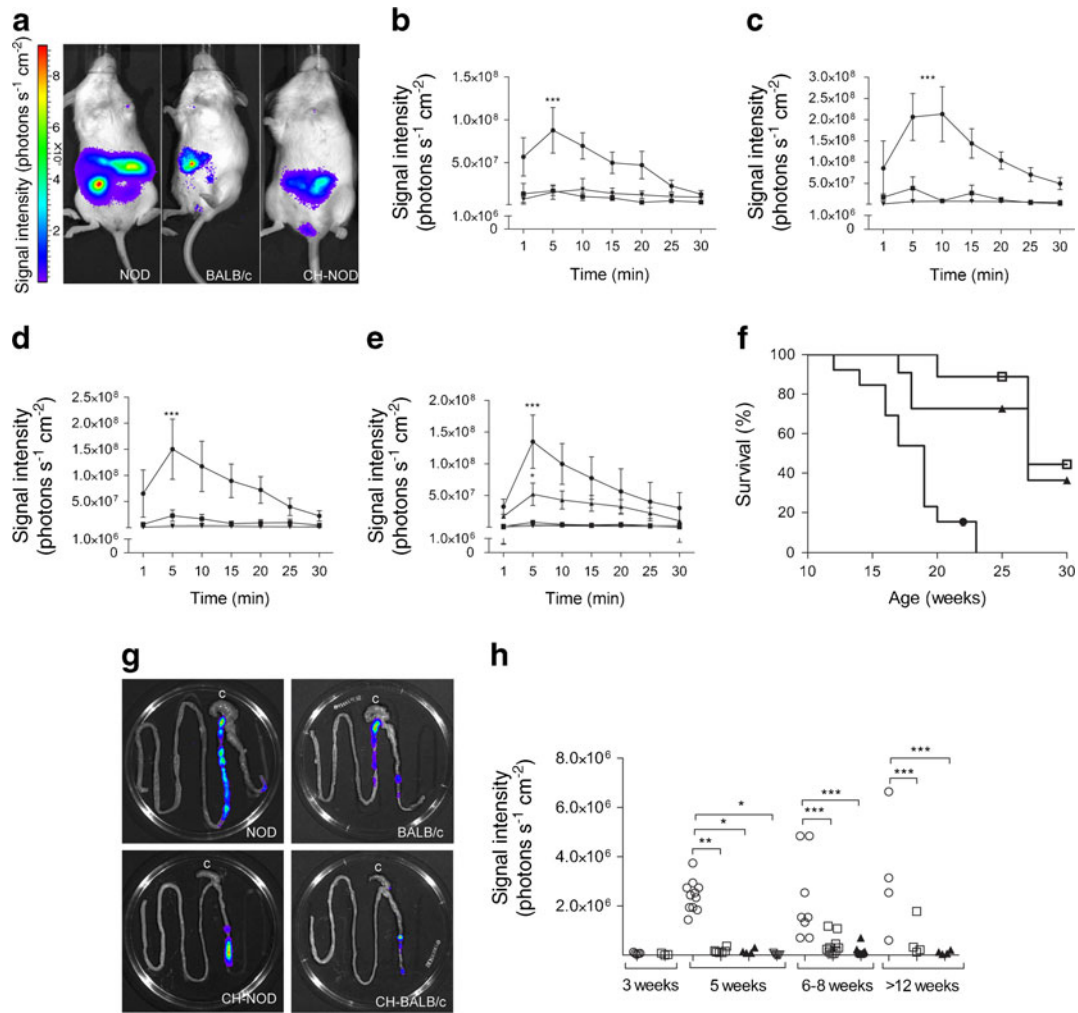


Fig. 1 RONS-dependent signal intensities in live NOD and BALB/c mice and in whole-gut mounts after intraperitoneal injection of the L-012 probe. **(a)** Representative images of 5-week-old mice on normal or CH diet (CH-NOD). **(b–e)** Mean signal intensities in the abdominal area of **(b)** 5-, **(c)** 7-, **(d)** 12- and **(e)** 20-week-old mice as a function of time; $n=6$ mice per group; $***p<0.001$ by one-way ANOVA. Black circles, NOD; black squares, BALB/c; black downward triangles, CH-NOD; black upward triangles, CH-NOD-DC (mice whose diet was changed from hydrolysate to normal chow at 12 weeks of age [only in **e**]). **(f)** Diabetes-free survival of female NOD mice on normal or CH diet; $n=8$ mice per group; $p<0.001$ by Mann–Whitney U test. Black

circle, NOD; black triangles, CH-NOD; white squares, CH-NOD-DC. **(g)** Whole-gut mounts of 5-week-old NOD and BALB/c mice on normal or CH diet. The small intestine is to the left of the caecum (marked c). **(h)** Mean signal intensity of the distal part of small intestine (ileum) in NOD and BALB/c mice of indicated ages, and the effect of diet in NOD mice. The effect of diet on BALB/c mice is included for 5-week-old animals. Each data point represents the value for an individual mouse; $*p<0.05$. $**p<0.01$ and $***p<0.001$. White circles, NOD; white squares, BALB/c; black triangles CH-NOD; white triangles, CH-BALB/c

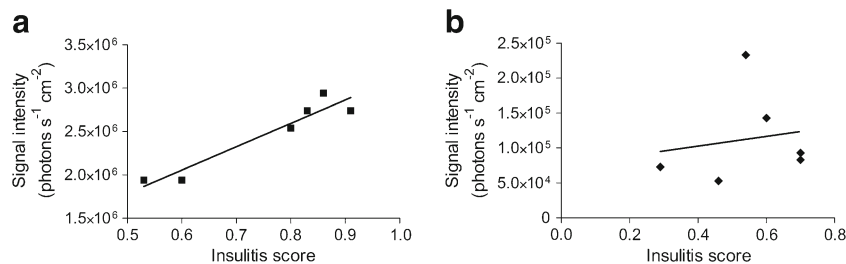
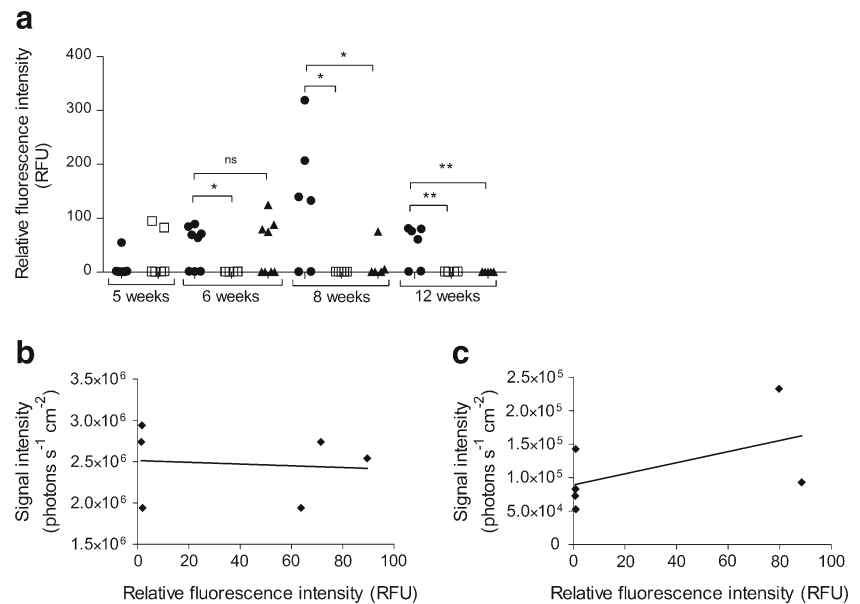


Fig. 2 Linear regression analysis of the correlation between RONS levels and insulinitis in NOD mice fed **(a)** normal chow ($R^2=0.911$) and **(b)** the CH diet ($R^2=0.027$). Individual mice were plotted for insulinitis

score (>30 islets per pancreas analysed) and RONS signal in the distal small intestine. **(b)** Note the different scale for insulinitis and RONS

Fig. 3 (a) Fluorescence intensities of serum samples from NOD (black circles), CH-diet-fed NOD (black triangles) and BALB/c (white squares) mice. Each data point represents an individual mouse tested. Relative fluorescence units (RFU) were calculated as the rate of signal (emitted light at 485–535 nm per s) in the sample relative to the signal given by normal serum; * $p < 0.05$ and ** $p < 0.01$. (b) Lack of correlation between serum FITC-dextran and intestinal RONS levels in NOD ($R^2 = 0.0009$) and (c) CH-diet-fed NOD mice ($R^2 = 0.290$)



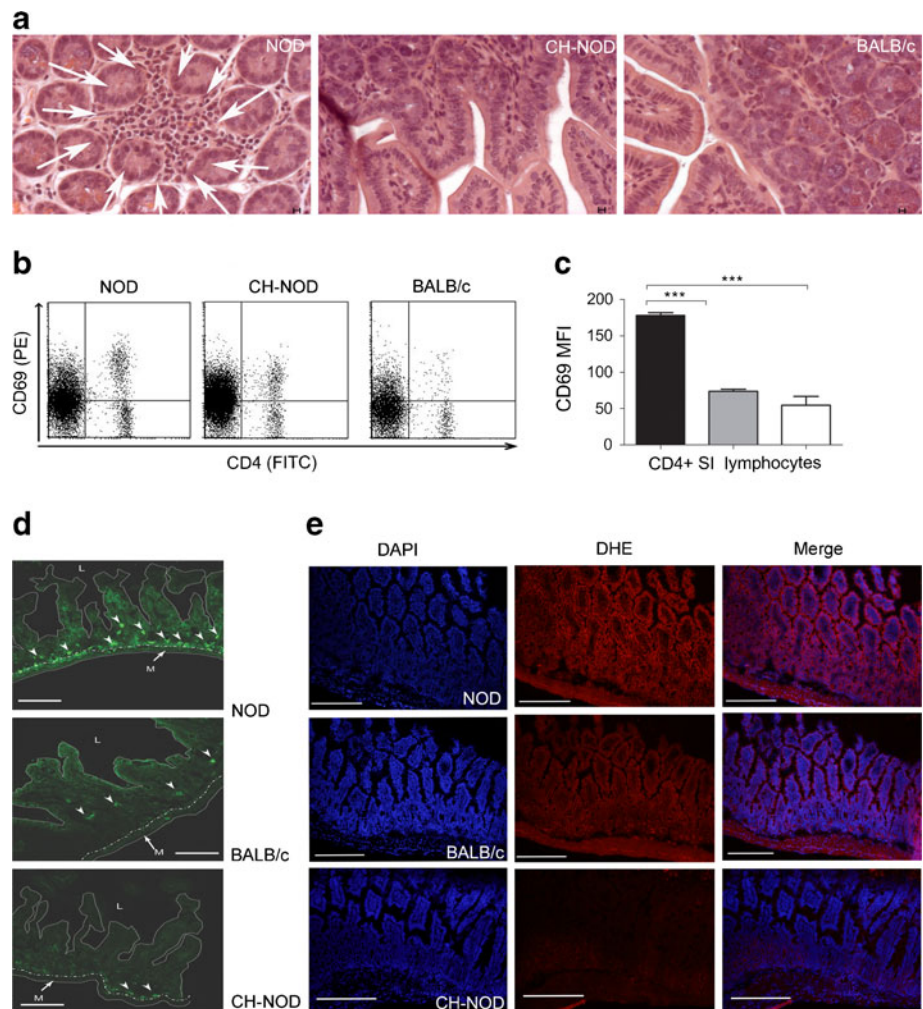
are part of the intracellular microbe killing machinery [24]. Epithelial cells also produce RONS, this production also being stimulated by microbial contacts [30]. We first studied sections of NOD ileum using conventional histological techniques, and found occasional small foci of accumulated lymphocytes and plasma cells in lamina propria (Fig. 4a); these foci were present in NOD mice fed normal chow diet, but not in those on the CH diet. In flow cytometry, T cells isolated from ileum showed higher CD69 expression in normal chow-fed NOD mice, suggesting a higher level of activation in this group (Fig. 4b,c). Immunostaining for myeloperoxidase revealed myeloid leucocytes, probably neutrophils, scattered in the lamina propria (Fig. 4d). Myeloperoxidase-expressing cells were frequent in the ileum of all NOD mice studied, but were less frequent on average in healthy BALB/c mice. In contrast, CH diet-fed NOD mice showed markedly fewer myeloperoxidase-expressing cells than NOD mice on normal chow (Table 1). To evaluate the role of epithelial cells in RONS production, we used in vivo staining with DHE. Strong DHE staining in the cytoplasm of epithelial cells was observed in the villi in NOD mice, indicating that these cells produced considerable amounts of RONS. NOD mice fed a CH diet showed reduced DHE staining, indicating reduced RONS production by the intestinal epithelium (Fig. 4e).

RONS production is associated with proinflammatory cytokine, antibacterial lectin and Th17 responses RONS production can exert autocrine and paracrine effects [31] on homeostasis and signalling of many cell types, thus promoting local inflammatory reactions and immune reactivity. Accordingly, Il1, Il6, Il18, Il23 and Il17 levels were all high in the ileum of NOD mice fed normal chow (Fig. 5a–e). Interestingly, this was associated with high expression of

bactericidal lectin *RegIII γ* (also known as *Reg3g*) (Fig. 5f), which is produced by gut epithelial cells in response to microbial colonisation [32]. Consistent with the increased local IL-17 production, ex vivo-stimulated T cells isolated from mesenteric lymph nodes produced more IL-17 in NOD mice fed normal diet than in NOD mice on the anti-diabetogenic CH diet (Fig. 5g–k).

A CH diet affects bacterial colonisation of the intestine As RONS are produced in response to contact with microbes and the CH diet is associated with lower RONS production, it was important to determine whether the diet-associated reduction of RONS production was associated with a qualitative or quantitative change in intestinal microbial communities. The CH diet diminished total bacterial content in the intestine (Fig. 6a,b). This affected all major groups of bacteria studied, but also induced qualitative changes in the composition of microbiota, as indicated by the G+C distribution of total bacterial DNA in per cent G+C profiling (Fig. 6c). qPCR analysis of six clusters of bacteria indicated that the CH diet affected the densities of bacteria belonging to Clostridial cluster XIVa more profoundly than that of *Bacteroides* spp., thus increasing the Bacteroidetes:Firmicutes ratio (Fig. 6d,e, ESM Fig. 1). In other clusters, smaller effects were detected, such as stimulation of Clostridial cluster IV and Coriobacteriaceae [33]. Interestingly, Clostridial cluster IV includes important probiotic and immunoregulatory bacteria [16] such as *Faecalibacterium prausnitzii* [34]. In contrast, the absolute numbers of *Lactobacilli* were suppressed with the CH diet (Fig. 6e). SFB colonisation was also determined in stool samples [35], but not found to be affected by the diet (ESM Table 4). Concentrations of short-chain fatty acids in luminal contents also reflected changes in the composition of microbiota, as butyrate (efficiently produced by certain

Fig. 4 (Immuno)histochemistry and flow cytometry of gut T cells. **(a)** Haematoxylin and eosin staining of NOD and BALB/c ileum showing (white arrows) a focus of leucocytes in the lamina propria of NOD mice on normal chow. Magnification $\times 40$; scale bar 5 μm . **(b)** Representative dot-plots of CD69 expression on CD4 T cells from gut wall. PE, phycoerythrin. **(c)** Mean fluorescence intensity (MFI) of CD69 expression on gut CD4 T cells as determined from individual mice; $n=5$; $***p<0.001$. Black bars, NOD mice; grey bars, BALB/c mice; white bars, CH-diet-fed NOD mice. **(d)** Myeloperoxidase immunostaining (green fluorescence), indicating the presence of neutrophil-like cells (arrowheads) in lamina propria (L, lumen; M, muscle layer). **(e)** Representative in vivo DHE staining (red) showing cytoplasmic reactivity in epithelial cells of the intestinal villi ($n=3$ mice per group). Sections of small intestine were counterstained with DAPI for nuclei. Magnification $\times 20$; scale bars 100 μm (**d**) and 200 μm (**e**)



firmicutes) and lactate concentrations were lower in the CH diet group (Fig. 6f–j).

*Casein hydrolysate diet treatment reduced *Ifng* and *Il17* in islets* The CH diet reduced RONS production in the ileum and Th17 immunity in gut-draining lymph nodes of NOD mice. To determine whether this reflects upon cytokine levels in islet infiltrates, we used laser capture microscopy to measure *Il17* (also known as *Il17a*) and *Ifng* transcripts from islet tissue prepared from frozen pancreatic sections (Fig. 7a). The CH diet was associated with reduced islet infiltration (Fig. 7b) and significantly reduced expression of *Il17* and *Ifng* (Fig. 7c) in islet infiltrates.

Discussion

The gut immune system, dietary factors and the composition of gut microbiota are important in the pathogenesis of type 1 diabetes [1, 3, 7, 20]. However, their involvement in disease pathogenesis is unlikely to be similar over the whole length of the gastrointestinal tract. In this study, we identified a site,

which appears to react to environmental changes during weaning with inflammatory activity and to involve T cell activation in the gut in the NOD mouse. Whole-gut imaging for RONS revealed increased RONS synthesis in the ileum of young, prediabetic NOD mice. This was associated with increased production of proinflammatory cytokines and T cell activation locally, with enhanced Th17 activity in the draining lymph nodes. The main producers of RONS appeared to be epithelial cells, consistent with the finding of strong expression of *RegIII γ* , an antibacterial peptide produced in a toll-like receptor-4-dependent manner by epithelial cells in response to bacterial colonisation [32]. Epithelial cell RONS production and increased T cell activation were diminished by the CH diet, which also reduced microbial colonisation and *RegIII γ* . Diminished microbial colonisation in the ileum secondary to the CH diet provides a potential new aspect of the mechanisms of diet-dependent regulation of diabetogenesis in type 1 diabetes [36].

According to previous in vitro and in vivo studies, epithelial cells in the intestine produce free radicals in response to contact with commensal bacteria [30]. Compared with more proximal parts of the gastrointestinal tract, the distal

Table 1 Myeloperoxidase staining of non-epithelial neutrophil-like cells

| Mouse | 1 | 2 | 3 | 4 | 5 | 6 |
|--------|-----|-----|-----|------|-----|-----|
| NOD | +++ | +++ | +++ | +++ | +++ | +++ |
| BALB/c | + | + | ++ | ++++ | ++ | |
| CH-NOD | + | + | + | | | |

Frozen sections of ileum were stained for myeloperoxidase expression and numbers of neutrophil-like cells staining positively were evaluated semi-quantitatively (+ to +++) by two independent investigators $p < 0.05$ for difference between NOD and CH-NOD

small intestine is the first to become colonised with increasingly diverse microbiota consisting of *Enterobacteriaceae* and obligate anaerobes, and, in rodents, of SFB [37]. Thus, production of RONS appears to be a necessary and physiological host response to contact with microbiota in the ileum. Production of RONS was also detectable in the ileum of healthy BALB/c mice; indeed, similar observations were made earlier by Kielland et al [27]. For this reason, we also chose BALB/c mice as controls for our initial studies on RONS and gut permeability. In studies of T cell cytokines, BALB/c mice were not an optimal match with NOD mice, due to their inherent Th2 dominance. However, our comparisons

of NOD mice on high- and low-risk diet are independent of BALB/c controls, and thus the association between diet, RONS and Th17 responses in the gut of NOD mice remains valid.

Gut barrier function was found to be compromised in normal NOD mice after weaning. This suggests dysregulated epithelial cell homeostasis involving impaired tolerance to microbes and dietary irritants [38]. The fact that NOD mice fed a CH diet had more intact barrier function is in strong support of this. A recent study in BB rats also indicates that peptides from CH combined with a protein-free diet improve gut barrier function [39]. Contact with microbial factors induces tolerance to toll-like receptor-4 signalling in epithelial cells of the neonatal small intestine, which protects epithelial cells from a deleterious inflammatory response [40]. Malfunction in these pathways results in aggravated responses to microbial colonisation, such as elevated *RegIII γ* and RONS production in the small intestine, and activates NF- κ B and cytokine production [24] locally. Interestingly, a study in BB rats found that diabetic animals had relatively more *Enterobacteriaceae* specifically in the ileum in parallel to higher levels of RONS [41].

In our NOD mouse colonies on a normal or CH diet, SFB [42] were present in equal amounts. Thus, the pronounced

Fig. 5 Profiles of cytokine and *RegIII γ* expression in ileum tissue, and of cytokine production by T cells in mesenteric lymph nodes. (a) Cytokine transcripts of *Il1*, (b) *Il6*, (c) *Il18*, (d) *Il23* (also known as *Il23a*) and (e) *Il17*, and of (f) *RegIII γ* in ileum tissue of NOD and BALB/c mice on a normal diet, and of NOD mice on a CH diet (CH-NOD). Values are mean \pm SEM; $n=4-5$ mice per group. (g) Secretion of IL-2, (h) IFN- γ , (i) IL-4, (j) IL-10 and (k) IL-17 by lymph node T cells during 48 h of stimulation with plate-bound anti-CD3 antibody in the same groups. Data are from two (a–f) and three (g–k) individual experiments; * $p < 0.05$. ** $p < 0.01$ and *** $p < 0.001$

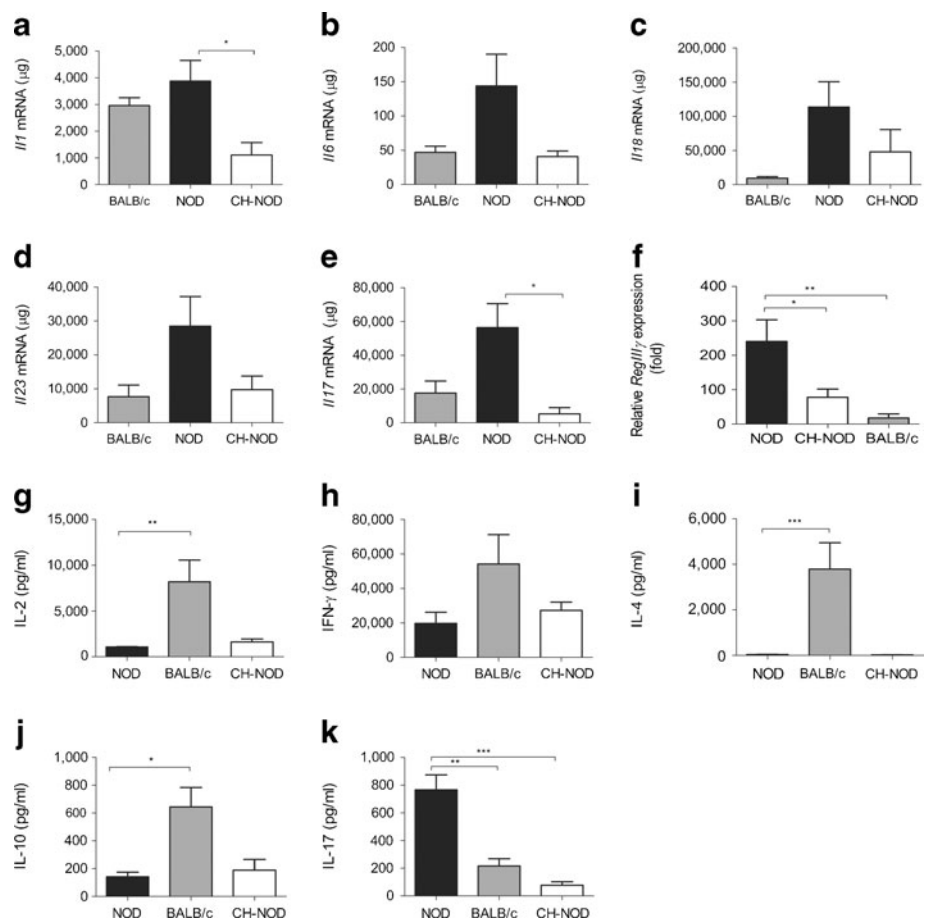
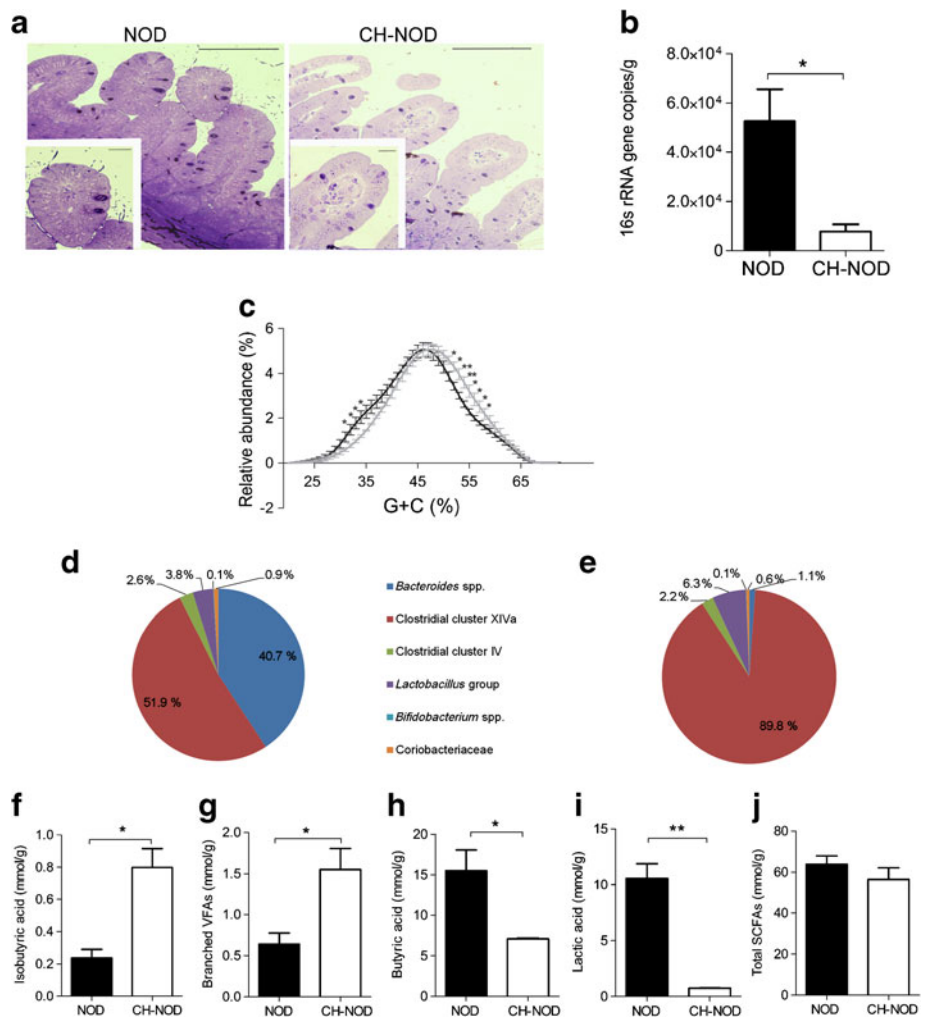


Fig. 6 Microbiota and their composition in NOD mice on normal or on a CH diet (CH-NOD). **(a)** Frequency of bacteria in the lumen of ileum samples fixed in methacrylate resin and stained with toluidine-blue. Magnification $\times 40$, scale bars 200 μm ; insets are magnified villi, magnification $\times 100$, scale bars 20 μm . **(b)** Total bacterial load (per g of intestinal content) as determined by copy number of 16S RNA-encoding DNA. **(c)** Distribution of the whole microbiota according to G+C profile as measured from unamplified total DNA. **(d–e)** Relative abundance of six bacterial clusters as determined by qPCR in **(d)** NOD and **(e)** CH-NOD mice. **(f–j)** Profile of short-chain fatty acids (SCFA) as indicated in intestinal contents of NOD and CH-NOD mice. Data **(b–j)** are from nine NOD and 15 CH-NOD mice, pooled to three biological replicates (from three and five mice, respectively); $*p < 0.05$ and $**p < 0.01$



IL-17 production in response to CD3-ligation in mesenteric lymph node cells of NOD mice fed a normal diet cannot be ascribed to different levels of SFB colonisation in the ileum. However, the total bacterial content in intestinal samples was much higher in mice fed a normal diet, consistent with the notion that various bacteria and the overall community

structure and quantity affect the IL-17 response, along with *RegIII γ* and the proinflammatory cytokine response. We propose that an aberrant epithelial immune response to microbial colonisation in NOD mice on normal chow occurs during weaning, inducing epithelial stress and local RONS production. This leads to inflammation and local T cell

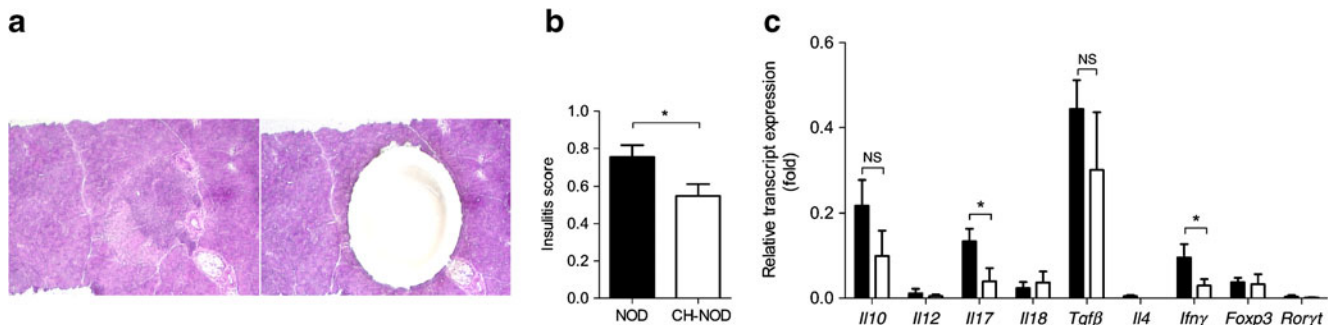


Fig. 7 Effect of CH diet on *Ifng* and *Il17* expression in islet infiltrates. **(a)** Laser capture microscopy sampling of frozen pancreatic sections to isolate RNA from infiltrated islets; $n = 30$ – 50 per pancreas. **(b)** Level of islet infiltration in 6-week-old NOD mice on a normal or CH diet (CH-NOD), expressed as insulinitis score; $n = 6$ mice per group with > 30 islets

per pancreas analysed. **(c)** Profiles of cytokine transcripts in islets of NOD (black bars) and CH-NOD (white bars) mice, determined by qPCR; $n = 5$ mice per group; $*p < 0.05$. *Il12*, also known as *Il12a*; *Tgf- β* , also known as *Tgfb1*

activation in the gut wall, to Th17 skewing in gut-draining lymph nodes and to accumulation of Th17 cells in islets, driving insulinitis and islet Th1 responses [43]. The CH diet controls all these phenomena, as well as gut leakiness in part, but the latter appears to be neither a prerequisite for RONS hyperproduction nor a necessary consequence of it.

Current, although limited, data in human type 1 diabetes cohorts suggests that butyrate- and lactate-producing bacteria are associated with protection from type 1 diabetes-related autoimmunity [7], and that children with type 1 diabetes-related autoimmunity suffer from an abundance of bacteria of the genus *Bacteroides* [8]. In addition, a recent study in the diabetes-prone BB model suggests that *Lactobacilli* were decreased in diabetic animals and restored by CH supplementation [39]. The role of *Lactobacilli* could thus be different between these two animal models of type 1 diabetes. If animal models represent different human type 1 diabetes disease phenotypes, the role of certain genera/species in individual cases of the disease may also be different.

In summary, we have identified a diet-dependent inflammatory reaction in the gut, which localises to the distal small intestine. With regard to the pathogenesis of islet autoimmunity, the consequences of the above could be enhanced co-stimulation during antigen presentation, the presentation of putative microbial mimicry peptides or proinflammatory conditioning of islet-destructive T cell responses in gut-draining lymph nodes. Alternatively, intestinal inflammation could promote the activation of islet-reactive T cells in pancreatic lymph nodes close to weaning [23]. Although the dissection of the above-mentioned effects on islet autoimmunity require further investigations, our results emphasise the importance of host \times dietary and host \times microbial interactions within the gut immune system in the pathogenesis of type 1 diabetes.

Acknowledgements We thank M. Linhala and M. Jaakkola (Department of Medical Microbiology and Immunology, University of Turku) and L. Ruotsala (Central Animal Laboratory, University of Turku) for technical assistance.

Funding This work was supported by grants from the Päivikki and Sakari Sohlberg Foundation (A. Hänninen), the Turku University Foundation (A. Hänninen), the Finnish Diabetes Research Foundation (to A. Hänninen, R. Toivonen), the Academy of Finland (to A. Hänninen, D. M. Toivola), the Sigrid Juselius Foundation (to D. M. Toivola) and the Turku Doctoral Programme for Biomedical Sciences (to M. N. Asghar).

Duality of interest The authors declare that there is no duality of interest associated with this manuscript.

Contribution statement RE and AH share responsibility for the conception and design of the study and experiments, data analysis and the writing of the manuscript. MNA, RT, LL, MS, DMT and EAFVT contributed to data acquisition and interpretation, and the drafting (MNA, RT, LL, MS) or revising (DMT, EAFVT) of the article. All authors have approved the final version of this manuscript to be published.

References

- Lefebvre DE, Powell KL, Strom A, Scott FW (2006) Dietary proteins as environmental modifiers of type 1 diabetes mellitus. *Annu Rev Nutr* 26:175–202
- Mojibian M, Chakir H, Lefebvre DE et al (2009) Diabetes-specific HLA-DR-restricted proinflammatory T cell response to wheat polypeptides in tissue transglutaminase antibody-negative patients with type 1 diabetes. *Diabetes* 58:1789–1796
- Knip M, Virtanen SM, Seppä K et al (2010) Dietary intervention in infancy and later signs of beta-cell autoimmunity. *N Engl J Med* 363:1900–1908
- Vaarala O, Ilonen J, Ruohtula T et al (2012) Removal of bovine insulin from cow's milk formula and early initiation of beta-cell autoimmunity in the FINDIA Pilot Study. *Arch Pediatr Adolesc Med* 166:608–614
- Virtanen SM, Kenward MG, Erkkola M et al (2006) Age at introduction of new foods and advanced beta cell autoimmunity in young children with HLA-conferred susceptibility to type 1 diabetes. *Diabetologia* 49:1512–1521
- Sorensen IM, Joner G, Jennum PA, Eskild A, Torjesen PA, Stene LC (2012) Maternal serum levels of 25-hydroxy-vitamin D during pregnancy and risk of type 1 diabetes in the offspring. *Diabetes* 61:175–178
- Brown CT, Davis-Richardson AG, Giongo A et al (2011) Gut microbiome metagenomics analysis suggests a functional model for the development of autoimmunity for type 1 diabetes. *PLoS One* 6:e25792
- de Goffau MC, Luopajarvi K, Knip M et al (2012) Fecal microbiota composition differs between children with beta-cell autoimmunity and those without. *Diabetes* 62:1238–1444
- Hooper LV, Littman DR, Macpherson AJ (2012) Interactions between the microbiota and the immune system. *Science* 336:1268–1273
- Vaarala O, Atkinson MA, Neu J (2008) The "perfect storm" for type 1 diabetes: the complex interplay between intestinal microbiota, gut permeability, and mucosal immunity. *Diabetes* 57:2555–2562
- Secondulfo M, Iafusco D, Carratu R et al (2004) Ultrastructural mucosal alterations and increased intestinal permeability in non-celiac, type 1 diabetic patients. *Dig Liver Dis* 36:35–45
- Westerholm-Ormio M, Vaarala O, Pihkala P, Ilonen J, Savilahti E (2003) Immunologic activity in the small intestinal mucosa of pediatric patients with type 1 diabetes. *Diabetes* 52:2287–2295
- Hadjiyanni I, Li KK, Drucker DJ (2009) Glucagon-like peptide-2 reduces intestinal permeability but does not modify the onset of type 1 diabetes in the nonobese diabetic mouse. *Endocrinology* 150:592–599
- Neu J, Reverte CM, Mackey AD et al (2005) Changes in intestinal morphology and permeability in the biobreeding rat before the onset of type 1 diabetes. *J Pediatr Gastroenterol Nutr* 40:589–595
- Alam C, Valkonen S, Palagani V, Jalava J, Eerola E, Hanninen A (2010) Inflammatory tendencies and overproduction of IL-17 in the colon of young NOD mice are counteracted with diet change. *Diabetes* 59:2237–2246
- Atarashi K, Tanoue T, Shima T et al (2011) Induction of colonic regulatory T cells by indigenous *Clostridium* species. *Science* 331:337–341
- Lee YK, Menezes JS, Umesaki Y, Mazmanian SK (2011) Proinflammatory T cell responses to gut microbiota promote experimental autoimmune encephalomyelitis. *Proc Natl Acad Sci U S A* 108(Suppl 1):4615–4622
- Slack E, Hapfelmeier S, Stecher B et al (2009) Innate and adaptive immunity cooperate flexibly to maintain host-microbiota mutualism. *Science* 325:617–620

19. Brugman S, Klatter FA, Visser JT et al (2006) Antibiotic treatment partially protects against type 1 diabetes in the Bio-Breeding diabetes-prone rat. Is the gut flora involved in the development of type 1 diabetes? *Diabetologia* 49:2105–2108
20. Wen L, Ley RE, Volchkov PY et al (2008) Innate immunity and intestinal microbiota in the development of type 1 diabetes. *Nature* 455:1109–1113
21. Alam C, Valkonen S, Ohls S, Tornqvist K, Hanninen A (2010) Enhanced trafficking to the pancreatic lymph nodes and auto-antigen presentation capacity distinguishes peritoneal B lymphocytes in non-obese diabetic mice. *Diabetologia* 53:346–355
22. Lee AS, Gibson DL, Zhang Y, Sham HP, Vallance BA, Dutz JP (2010) Gut barrier disruption by an enteric bacterial pathogen accelerates insulinitis in NOD mice. *Diabetologia* 53:741–748
23. Turley SJ, Lee JW, Dutton-Swain N, Mathis D, Benoist C (2005) Endocrine self and gut non-self intersect in the pancreatic lymph nodes. *Proc Natl Acad Sci U S A* 102:17729–17733
24. Fialkow L, Wang Y, Downey GP (2007) Reactive oxygen and nitrogen species as signaling molecules regulating neutrophil function. *Free Radic Biol Med* 42:153–164
25. Brumell JH, Burkhardt AL, Bolen JB, Grinstein S (1996) Endogenous reactive oxygen intermediates activate tyrosine kinases in human neutrophils. *J Biol Chem* 271:1455–1461
26. Schreck R, Rieber P, Baeuerle PA (1991) Reactive oxygen intermediates as apparently widely used messengers in the activation of the NF-kappa B transcription factor and HIV-1. *EMBO J* 10:2247–2258
27. Kielland A, Blom T, Nandakumar KS, Holmdahl R, Blomhoff R, Carlsen H (2009) In vivo imaging of reactive oxygen and nitrogen species in inflammation using the luminescent probe L-012. *Free Radic Biol Med* 47:760–766
28. Zangani M, Carlsen H, Kielland A et al (2009) Tracking early autoimmune disease by bioluminescent imaging of NF-kappaB activation reveals pathology in multiple organ systems. *Am J Pathol* 174:1358–1367
29. Symonds EL, Riedel CU, O'Mahony D, Lapthorne S, O'Mahony L, Shanahan F (2009) Involvement of T helper type 17 and regulatory T cell activity in *Citrobacter rodentium* invasion and inflammatory damage. *Clin Exp Immunol* 157:148–154
30. Kumar A, Wu H, Collier-Hyams LS et al (2007) Commensal bacteria modulate cullin-dependent signaling via generation of reactive oxygen species. *EMBO J* 26:4457–4466
31. Zangar RC, Bollinger N, Weber TJ, Tan RM, Markillie LM, Karin NJ (2011) Reactive oxygen species alter autocrine and paracrine signaling. *Free Radic Biol Med* 51:2041–2047
32. Cash HL, Whitham CV, Behrendt CL, Hooper LV (2006) Symbiotic bacteria direct expression of an intestinal bactericidal lectin. *Science* 313:1126–1130
33. Malinen E, Krogius-Kurikka L, Lyra A et al (2010) Association of symptoms with gastrointestinal microbiota in irritable bowel syndrome. *World J Gastroenterol* 16:4532–4540
34. Fujimoto T, Imaeda H, Takahashi K et al (2012) Decreased abundance of *Faecalibacterium prausnitzii* in the gut microbiota of Crohn's disease. *J Gastroenterol Hepatol* 28:613–619
35. Kriegel MA, Sefik E, Hill JA, Wu HJ, Benoist C, Mathis D (2011) Naturally transmitted segmented filamentous bacteria segregate with diabetes protection in nonobese diabetic mice. *Proc Natl Acad Sci U S A* 108:11548–11553
36. Vaarala O (2011) The gut as a regulator of early inflammation in type 1 diabetes. *Curr Opin Endocrinol Diabetes Obes* 18:241–247
37. Davis CP, Savage DC (1974) Habitat, succession, attachment, and morphology of segmented, filamentous microbes indigenous to the murine gastrointestinal tract. *Infect Immun* 10:948–956
38. Renz H, Brandtzaeg P, Hornef M (2012) The impact of perinatal immune development on mucosal homeostasis and chronic inflammation. *Nat Rev Immunol* 12:9–23
39. Visser JT, Bos NA, Harthoorn LF et al (2012) Potential mechanisms explaining why hydrolysed casein based diets outclass single amino acid based diets in the prevention of autoimmune diabetes in diabetes prone BB rats. *Diabetes Metab Res Rev* 28:505–513
40. Chassin C, Kocur M, Pott J et al (2010) miR-146a mediates protective innate immune tolerance in the neonate intestine. *Cell Host Microbe* 8:358–368
41. Valladares R, Sankar D, Li N et al (2010) *Lactobacillus johnsonii* N6.2 mitigates the development of type 1 diabetes in BB-DP rats. *PLoS One* 5:e10507
42. Ivanov II, Atarashi K, Manel N et al (2009) Induction of intestinal Th17 cells by segmented filamentous bacteria. *Cell* 139:485–498
43. Bending D, de la Pena H, Veldhoen M et al (2009) Highly purified Th17 cells from BDC2.5NOD mice convert into Th1-like cells in NOD/SCID recipient mice. *J Clin Invest* 119:565–572